# Simulations of blast wave propagation in open space that require adaptive mesh refinement

Tae-jun Roh, Young-hun Lee, Jack J. Yoh
Department of Mechanical & Aerospace Engineering, Seoul National University
Seoul, Korea 151-742

## 1 Introduction

When detonation occurs in open space areas, the energy of reaction is released instantly in short time and high pressure dense product gas is produced and expanded. The impulsive energy released quickly reaches equilibrium with the environment by expansion in air while producing multiple shock waves in the form of blast wave. The blast wave traveling in open space follows a Friedlander waveform: instantaneously increasing to a maximum peak pressure well above the ambient pressure and then decaying exponentially away from the source of explosion.

Previous works in blast wave simulations provided an empirical equation for predicting peak pressure using explosive weight and standoff distance [1]. To accurately simulate and predict the effects of blast wave propagation pertaining to specific environments, a large-scale integrated hydrodynamic simulation that can handle very large spatial dimensions is required. The reaction length associated with a source detonator is typically a few orders of magnitude shorter than open space domain, and thus a necessary mesh refinement suitable for blast wave propagation must be considered into one's numerical method. Also to minimize computational load in tracking interface between hot product gas and ambient air, an integrated equation of state that considers both materials must be developed.

In this work, numerical simulations of a spherical charge detonation in open air areas are conducted and verified against the experimental measurements.

## 2 Experiment: a point source detonation in open space

A spherical RDX of weight 5.6 kg [2] was detonated at a height of 1.8 m from the ground, allowing the explosive wave to reach and reflect from the ground. The characteristics of the blast wave at each segment of axial location were recorded by pressure sensors arranged in 20 m from the source as shown in Fig. 1.

**Correspondence to: jjyoh@snu.ac.kr**

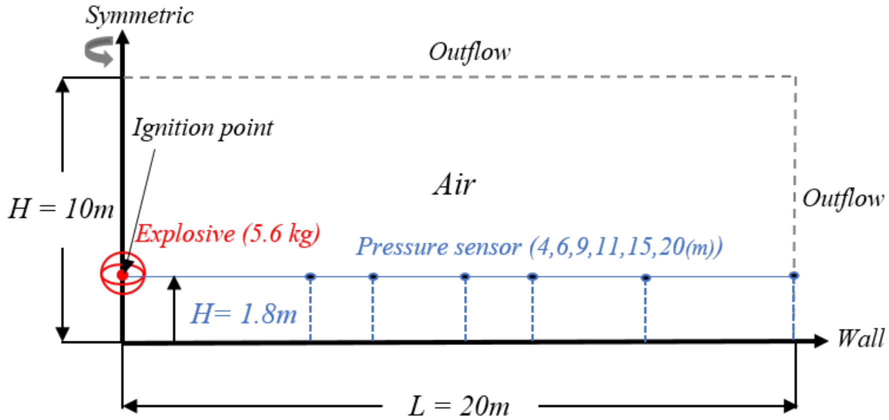


Figure 1. Air blast experiment and simulation setup

## 3 Numerical Formulation

### 3.1 Governing Equation

The governing equations involving mass, momentum, energy conservation, and reaction progress are explicitly written for a 2D axisymmetric cylindrical (φ=1) and rectangular (φ=0) system as follows: [3]

$$\frac{\partial U}{\partial t}+\frac{\partial E}{\partial x}+\frac{\partial F}{\partial y}=RHS \tag{1}$$

$$U=\left[\rho,\rho v_1,\rho v_2,\rho E,\rho\lambda\right]^{\mathrm{T}} \tag{2}$$

$$F=\left[\rho v_1,\rho v_1^2+P,\rho v_1 v_2,v_1\left(\rho E+P\right),\rho\lambda v_1\right]^{\mathrm{T}} \tag{3}$$

$$G=\left[\rho v_2,\rho v_1 v_2,\rho v_2^2+P,v_2\left(\rho E+P\right),\rho\lambda v_2\right]^{\mathrm{T}} \tag{4}$$

$$RHS=\left[0,0,0,0,\rho\dot{w}\right]^{\mathrm{T}}+R \tag{5}$$

$$R=-\frac{\varphi}{x}\left[\rho v_1,\rho v_1^2,\rho v_1 v_2,v_1\left(\rho E+P\right),\rho v_1\lambda\right]^{\mathrm{T}} \tag{6}$$

Here, ρ is the density, $v_1$ and $v_2$ are the velocity components in the x-, y- directions, respectively, $E$ is the total energy per unit mass, $\lambda$ is the mass fraction of the product, and P is the hydrostatic pressure. To solve the explosive detonation process and blast wave propagation and reflection, third-order Convex essentially non-oscillatory (ENO) method and third-order Runge-Kutta (RK) method are used for spatial and time integration, respectively. A level set equation is used to track the interface and ghost fluid method is utilized for determining the conditions of materials at contact.

## 3.2 Reaction rate law and equation of state (EOS)

For simulating detonation of RDX, modified Ignition & Growth model is utilized for explosive chemical kinetics expressed as Eq. (7). In addition, Mie-Gruneisen EOS and JWL EOS shown in Eq. (8) and Eq. (9) are used to analyze the unreacted and reacted explosive pressure, respectively. For air, the ideal gas law is adopted. The EOS parameters of explosive (RDX) and air are listed in the Table 1. [2]

$$\dot{w} = I(1-\lambda)\mu^{a}\big|_{0\le\lambda\le 0.01} + G(1-\lambda)P^{b}\big|_{0.01\le\lambda\le 1} \;\; ; \;\; \mu = \frac{\rho}{\rho_0} - 1 \tag{7}$$

$$P_{\text{unreacted}} = P_{\text{H}} + \Gamma\rho(\text{e} - \text{e}_H); \; V = \frac{\rho_0}{\rho} \tag{8}$$

$$P_{\text{reacted}} = A_1\left(1 - \frac{w_1}{R_{11}V}\right)e^{-R_{11}V} + B_1\left(1 - \frac{w_1}{R_{12}V}\right)e^{-R_{12}V} + w_1\frac{E}{V} \;\; ; \; V = \frac{\rho_0}{\rho} \tag{9}$$

Table 1: Modeling constants for explosive and air.

| Parameters | RDX | Air |
|---|---|---|
| $\rho_0$ (kg/m$^3$) | 1830 | 1.16 |
| $C_0$ (m/s) | 2406 | - |
| $S$ | 1.89 | - |
| $\Gamma$ | 0.99 | 1.4 |
| $A$ (GPa) | 628.6 | - |
| $B$ (GPa) | 4.80 | - |
| $R_1$ | 5.10 | - |
| $R_2$ | 1.30 | - |
| $\omega$ | 0.086 | - |

## 3.3 Adaptive mesh refinement (AMR) for handling open space computing

To simultaneously simulate the point source detonation and its blast wave propagation, cell-based AMR is implemented to allocate required computational resources at regions where high mesh resolution is critical. The mesh division proceeds prior to calculating the fluxes. The difference of physical quantities such as ρ (density), P (pressure), and E (internal energy) are calculated for all existing cells to determine which region requires a finer mesh for accurately capturing the physical length scale associated with the transient zone. The refined cell is removed if it is no longer required.

The reaction length of considered explosive is about 5 mm, and the mesh size must be less than the reaction length. At the same time, computational domain of open space is as large as 20 meters in length and 10 meters in height. The AMR technique developed for this purpose uses 2 mm mesh size in the reaction zone that moves with blast wave propagation while a coarse mesh of 64 mm is used otherwise as shown in Fig. 2.

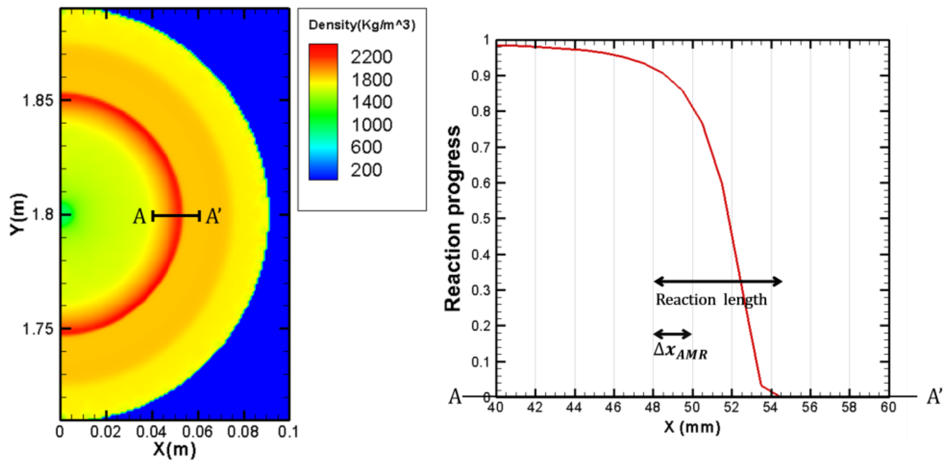


Figure 2. Left: point source detonation process shown density contour. Right: reaction progress shown with AMR minimum mesh size and reaction length.

### 3.4 Integration of two different equations of state

Level-set method and ghost fluid method are used to track interface and determine boundary conditions between two distinct materials since EOS and states are different in each material. When detonation process is completed, and the EOS of explosive detonation products shown in Eq. (9) is equal to the ideal gas equation in air, two independent EOS are no longer necessary. In order to reduce the computing load for open space area, the following integration technique is used. In Eq. (9), contributions from each of the three right-hand-side terms are plotted in Fig. 3, and labeled as A term, B term, and C term. When density and pressure drop below certain values, which are usually a tenth of initial density and corresponding pressure, A term and B term do not contribute while the remaining C term becomes most effective. Such JWL EOS finally converges to ideal gas law with an added heat of detonation. Therefore, when the highest density and pressure in simulation are below these values, $\rho^*$ and $P^*$, the integration of EOS is performed.

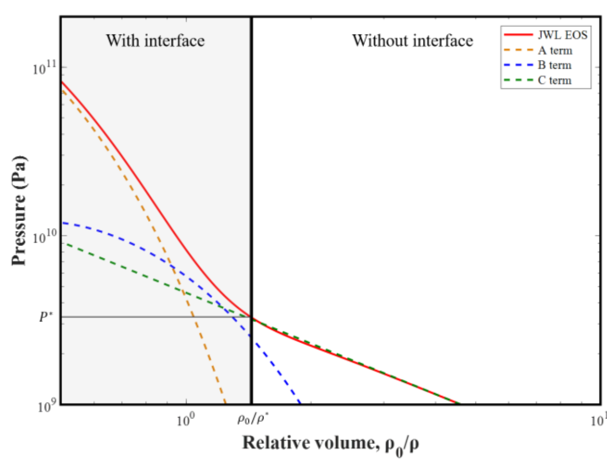


Figure 3. JWL EOS showing critical $P^*$ and $\rho^*$ for integration

## 4 Results and discussion

The simulation of the point source detonation followed by blast wave propagation in open space (20 meter by 10 meter) area is performed, and the results are compared against experiments. The initial conditions shown in Fig. 1 are used. As blast wave travels, the computational mesh is finely divided to capture the transients associated with the transient zone. Figure 5 shows mesh refinement process and the pressure contour that includes incident wave propagation with subsequent wave interactions with reflected waves. The number of maximum mesh in calculation was approximately 8,388,608. The comparison of pressure data from simulation and experiments is shown at Fig. 4. We can confirm that the first peak is from incident wave and the second peak is from reflected wave. Table 2 summarizes the peak pressure and impulse at six distinct sensor locations. The comparison of calculation with measurement is within 3.5 % error at peak pressures while impulse had less than 6.8 % discrepancy in quantitative comparison.

In conclusion, numerical methods consisted with AMR and integration of EOS are adapted into hydro-dynamic in-house code. By the solver, both processes of explosive detonation and blast wave propagation were successively simulated. Furthermore, it is validated by comparing the experimental data.

Table 2: Peak pressure and Impulse comparison

| | Peak pressure(Pa) | | Error(%) | Impulse(Pa*s) | | Error(%) |
|---|---|---|---|---|---|---|
| | experiment | simulation | | experiment | simulation | |
| 4m | 147200 | 151100 | 2.64 | 90.1647 | 90.6250 | 0.51 |
| 6m | 128400 | 125870 | 1.97 | 82.2594 | 83.7860 | 1.85 |
| 9m | 117024 | 115440 | 1.35 | 64.0226 | 67.5760 | 5.87 |
| 11m | 117640 | 113640 | 3.40 | 62.2581 | 61.7210 | 1.87 |
| 15m | 113330 | 109440 | 3.43 | 50.1281 | 52.6930 | 5.11 |
| 20m | 108970 | 106250 | 2.49 | 42.5657 | 45.4830 | 6.85 |

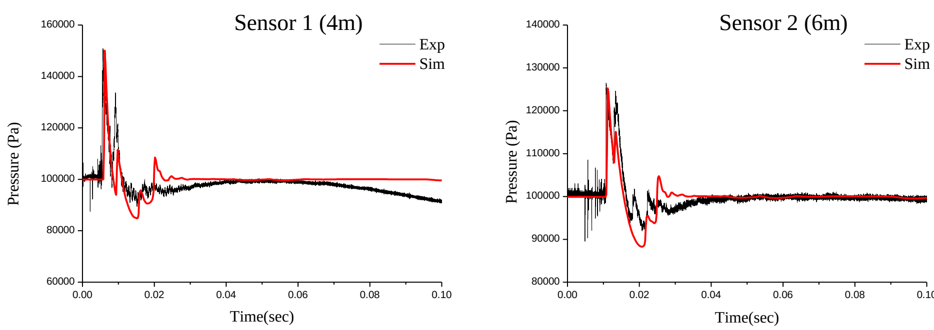


Figure 4. Comparison of pressure measurement and simulation at 2 sensor locations (4m, 6m). Experimental data (black line) and simulation results (red line).

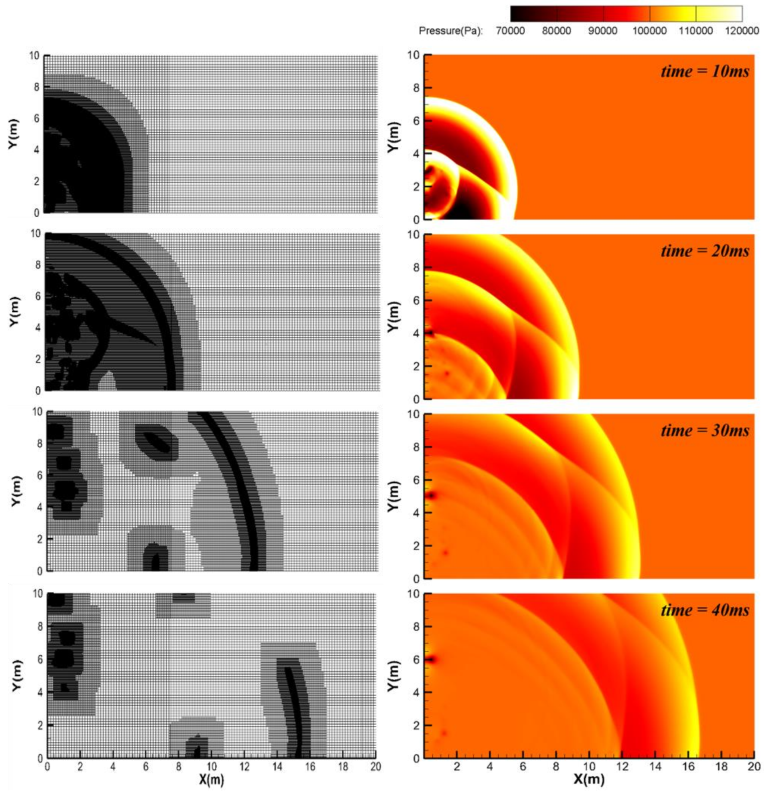


Figure 5. Left: AMR mesh. Right: pressure contour at 10, 20, 30, 40 ms

## References

[1] Kingery CN, Bulmash G. (1984). Airblast parameters from TNT spherical air burst and hemispherical surface burst, Report ARBL-TR-02555, U.S. Army BRL, Aberdeen Proving Ground, MD

[2] Baek D, Kim B, Yoh JJ. (2018). Modelling the effects of aluminum and ammonium perchlorate addition on the detonation of the high explosives HMX and RDX. J. Appl. Phys. 124: 215905

[3] Kim W, Gwak M, Lee Y, Yoh JJ. (2018) A two-phase model for aluminized explosives on the ballistic and brisance performance. J. Appl. Phys. 123: 055902.

[4] Lee Y, Lee W, Gwak M, Kim K, Yoh JJ. (2018). A reactive flow simulation for the anisotropic ignition of an explosive crystal using adaptive mesh refinement. J. Appl. Phys 124: 145903.

[5] Donahue L, Zhang F, Ripley RC. (2013). Numerical models for afterburning of TNT detonation products in air. Shock Wave. 23: 559-573.

[6] Gwak M, Lee Y, Kim K, Yoh JJ. (2015). Deformable wall effects on the detonation of combustible gas mixture in a thin-walled tube. Int. J. Hydrogen Energ. 40: 3006.

[7] Schnetter E, Scott HH, Hawke I. (2004). Evolutions in 3D numerical relativity using fixed mesh refinement. Class. Quantum Grav. 21: 1465–1488.